Published in final edited form as:
Neuroscience. 2015 August 06; 300: 493–507. doi:10.1016/j.neuroscience.2015.05.046.

DYSREGULATED TNFα PROMOTES CYTOKINE PROTEOME PROFILE INCREASES AND BILATERAL OROFACIAL HYPERSENSITIVITY

F. MA, **L. ZHANG**, **H. S. OZ**, **M. MASHNI**, and **K. N. WESTLUND***
Department of Physiology, College of Medicine, University of Kentucky, Lexington, KY 40536-0298, United States

Abstract

Background: Tumor necrosis factor alpha (TNFα) is increased in patients with headache, neuropathic pain, periodontal and temporomandibular disease. This study and others have utilized TNF receptor 1/2 (TNFR1/2) knockout (KO) animals to investigate the effect of TNFα dysregulation in generation and maintenance of chronic neuropathic pain. The present study determined the impact of TNFα dysregulation in a trigeminal inflammatory compression (TIC) nerve injury model comparing wild-type (WT) and TNFR1/2 KO mice.

Methods: Chromic gut suture was inserted adjacent to the infraorbital nerve to induce the TIC model mechanical hypersensitivity. Cytokine proteome profiles demonstrated serology, and morphology explored microglial activation in trigeminal nucleus 10 weeks post.

Results: TIC injury induced ipsilateral whisker pad mechanical allodynia persisting throughout the 10-week study in both TNFR1/2 KO and WT mice. Delayed mechanical allodynia developed on the contralateral whisker pad in TNFR1/2 KO mice but not in WT mice. Proteomic profiling 10 weeks after chronic TIC injury revealed TNFα, interleukin-1alpha (IL-1α), interleukin-5 (IL-5), interleukin-23 (IL-23), macrophage inflammatory MIP-1β(MIP-1β), and granulocyte–macrophage colony-stimulating factor (GM-CSF) were increased more than 2-fold in TNFR1/2 KO mice compared to WT mice with TIC. Bilateral microglial activation in spinal trigeminal nucleus was detected only in TNFR1/2 KO mice. p38 mitogen-activated protein kinase (MAPK) inhibitor and microglial inhibitor minocycline reduced hypersensitivity.

Conclusions: The results suggest the dysregulated serum cytokine proteome profile and bilateral spinal trigeminal nucleus microglial activation are contributory to the bilateral mechanical hypersensitization in this chronic trigeminal neuropathic pain model in the mice with TNFα

*Corresponding author. Address: Department of Physiology, MS-508, College of Medicine, University of Kentucky, Lexington, KY 40536-0298, United States. Tel: +1-859-323-3668; fax: +1-859-323-1070. kwhigh2@uky.edu (K. N. Westlund).

AUTHORS' CONTRIBUTIONS

All authors have read and approved the final manuscript. FM carried out behavioral tests, histological study, plotted figures and drafted the manuscript. LZ participated in behavioral tests, proteomic profile analysis and histological study as well as image analysis. HO performed, analyzed, and interpreted the proteomic assay. MM participated in proteome profile analysis and histological study as well as image analysis. LZ and MM prepared the figures and tables. FM, LZ and HO edited the text. KNW supervised the study, edited the text and figures for the submissions.

COMPETING OF INTERESTS

The authors declare no financial or relationships that might lead to conflict of interests.

dysregulation. Data support involvement of both neurogenic and humoral influences in chronic neuropathic pain.

Keywords

trigeminal inflammatory compression; neuropathic pain; mechanical allodynia; microglia; MAPK; minocycline

BACKGROUND

Tumor necrosis factor alpha (TNFα) is an inflammatory mediator produced not only by activated macrophages, CD4+ lymphocytes, and NK cells, but also by neurons, Schwann cells, astroglia, and microglia (Gregersen et al., 2000; Locksley et al., 2001). ATP released from nerve endings or leaked from damaged cells activates p38 or extracellular-signal-regulated kinase (ERK)1/2 resulting in release of TNFα (Hide et al., 2000). This proinflammatory chemokine has multiple actions including cytolysis, lymphocyte recruitment, and initiation of cascades of other proinflammatory cytokines/chemokines (Kreutzberg, 1996; Woolf et al., 1997). TNFα stimulation of nerve endings alters neuronal excitability and has been implicated in the mechanical allodynia associated with development of intractable neuropathic pain (Wagner and Myers, 1996; Sorkin and Doom, 2000; Empl et al., 2001; Sommer et al., 2001; Thacker et al., 2007; Uceyler et al., 2007; Ludwig et al., 2008).

The biologic activities of TNFα are mediated through two TNF gene family receptors (TNFR), the widely expressed TNFR1 and the limited constitutively expressed TNFR2. The main effect of TNFR1 is related to apoptosis whereas TNFR2 is associated with cell survival (Andrade et al., 2011). Feedback control maintained after the full-length membrane-spanning TNFα (mTNFα) is cleaved by the inducible TNF converting enzyme (TACE) to release the diffusible peptide and soluble TNFα (sTNFα) (Fang et al., 2006). TNFα is increased in trigeminal ganglia and temporomandibular joint (TMJ) in its tissue binding protein format in the complete Freund's adjuvant (CFA)-induced rat TMJ inflammation model (Spears et al., 2005). Increases in TNFα are evident in cerebrospinal fluid (CSF) and plasma of rats with spinal level spared nerve injury models (Ren et al., 2011). Successful alleviation of neuropathic pain with a gene therapy silencing TNF expression has been demonstrated (Ogawa et al., 2014).

Further examination of TNF dysfunction as a potentiator of orofacial neuropathic pain is warranted since TNFα levels in serum and CSF have been correlated with pain status in patients with other neuropathies (Koch et al., 2007; Uceyler et al., 2007; Ludwig et al., 2008). Trigeminal neuropathic pain is commonly seen following trigeminal nerve damage after surgical procedures or maxillofacial injuries (Becerra et al., 2006). Developing new models for study and new targets for better pharmacological treatment of orofacial pain is essential since for many patients neuropathic pain is continuous and/or intractable. In animal studies, chromic gut suture, CFA oxygel, and coral snake venom have been applied to trigeminal nerve branches to cause nerve inflammation and hypersensitivity of the orofacial area (Benoliel et al., 2002; An et al., 2011). We developed a mouse model of continuous,

chronic facial pain induced by inserting chromic gut suture under the infraorbital nerve to produce slight compression and chemical irritation. The histology confirmed mild axonal trauma, inflammation, and disruption of myelin were present among axons immediately adjacent to the suture (Ma et al., 2012).

In the present study, it was hypothesized that dysregulated TNFα contributes to the development of chronic neuropathic pain at both peripheral and central sites. The injury activates neurons in the trigeminal ganglion and microglial cells in the spinal trigeminal nucleus contributing to mechanical hypersensitivity on the whisker pad. Since microglia are one source of TNFα eliciting the inflammatory responses in the CNS (Stoll and Jander, 1999), it is likely that reciprocal activation of neurons and microglia centrally by TNFα induce mouse whisker pad allodynia in the trigeminal nerve injury model. Intrathecal injection of TNFα has been shown to produce thermal hyperalgesia and mechanical allodynia (Kawasaki et al., 2008). TNFα is theoretically promoting somatic or orofacial hypersensitivity acting through TNFR1 and TNFR2 receptors. CFA and formalin do not provoke typical nociceptive responses in TNFR1 or 2 knockout (KO) mice (Zhang et al., 2011). TNFα enhanced excitatory synaptic transmission in spinal lamina II neurons was minimal in the absence of TNFR1 and TNFR2 in short-term studies. Thus, support is increasing in understanding TNFα's contribution to the development of neuropathic pain (Marchand et al., 2005), and that soluble TNFR1 and R2 can neutralize circulating TNFα to alleviate thermal hyperalgesia or mechanical allodynia induced by peripheral nerve injury in most conditions (Sommer et al., 1998; Schafers et al., 2003).

In the present study, the potential of other proinflammatory cytokines as factors contributory to chronic pain was investigated in the absence of the TNF receptors in TNFR1/2 KO mice. The chronic trigeminal inflammatory compression (TIC) nerve injury model was utilized with mechanical allodynia that persisted chronically through at least 10 weeks. We reported previously that serum TNFα was elevated 8-fold in TNFR1/2 KO mice after an initial CFA induced inflammation became chronically recurrent (15 weeks) following a second insult (colitic mustard oil), while wild-type (WT) controls recover after one week (Westlund et al., 2012). Serum TNFα is also strikingly elevated in TNFR1/2 KO mice after intraperitoneal lipopolysaccharide (LPS) injection in comparison with either TNFR1 or TNFR2 KO mice in another study (Peschon et al., 1998).

In the present study, mechanical hypersensitivity was tested in the TNFR1/2 KO mice with TIC injury for comparison to WT mice throughout the 10-week study. Accompanying alterations in serum TNFα and other cytokines/chemokines in this chronic pain model were analyzed at 10 weeks. Microglial activation in both sides of trigeminal nucleus was explored. Potential mechanisms for the mechanical allodynia were tested using drugs targeting microglia and the p38 mitogen-activated protein kinase (MAPK) signaling pathway. Discussion follows about the involvement of both humoral and neurogenic influences of TNFα in the development of chronic neuropathic pain.

EXPERIMENTAL PROCEDURES

Animals

All experiments were carried out in accordance with the Guidelines of the National Institutes of Health (NIH) regarding the care and use of animals for experimental procedures. Protocols were approved by the Institutional Animal Care and Use Committee at the University of Kentucky.

The mice were male WT (B6129SF2/J) and TNFR1/2 KO (B6129S-Tnfrsf1a^{tm1Imx} Tnfrsf1b^{tm1Imx}/J) (Jackson Laboratory). The mice weighing 20–30 g at the beginning of the study were placed in microisolators and accommodated in ventilated animal housing with a reversed 10/14-h dark/light cycle.

Surgical induction of the TIC injury model

Mice were anesthetized with sodium pentobarbital (70 mg/kg, i.p.), and all surgeries were performed with the aid of a surgical microscope in sterile conditions. The hair over the head was shaved and each mouse fixed on a stereotaxic frame for surgery. Artificial tears were applied to both eyes to prevent dryness. A 15-mm longitudinal incision was made in skin along the midline of the head. The orbital muscle was gently dissected from the bone and gently retracted from the orbit. The infraorbital nerve was located ~5 mm deep in the orbital cavity lying within the infraorbital fissure. The infraorbital nerve was dissected free from the bone and a 2-mm length of chromic gut suture (6–0) was inserted between the infraorbital nerve and the maxillary bone as described previously (Ma et al., 2012). The nerve was not dissected in the surgical sham mice. The skin incision was then closed with 5–0 nylon suture.

Pain related behavioral assessment

Mice were habituated before experiments. The 50% mechanical withdrawal threshold (grams, g) of the whisker pad was assessed with a modified up-and-down method using a set of von Frey filaments ((4.74) 6.0 g; (4.31) 2.0 g; (4.08) 1.0 g; (3.61) 0.4 g; (3.22) 0.16 g; (2.83) 0.07 g; (2.36) 0.02 g; (1.65) 0.008 g; Stoelting, Wood Dale, IL, USA) (Chaplan et al., 1994). Each filament was applied three to five times at intervals of a few seconds. If head withdrawal or front paw swipe toward the face was observed at least three times with filament probing, the mouse was considered responsive to that filament. When the mouse was responsive to one filament, the next weaker one was applied. The next stronger filament was applied if there was no response. The whisker pad was tested on both sides. The examiner was blinded to the groups of mice tested. The testing method allowed calculation using the published curve-fitting algorithm. There can be up to 2-g variation in the mechanical threshold in normal mice with this test. The threshold is decreased during the 3 weeks recovery from surgery in both the TIC injury and sham surgery group.

Drug administration

Behavioral changes were monitored for 1 h in week 9 after a single administration of minocycline hydrochloride (30 mg/kg). Minocycline is a microglial activation inhibitor (Sigma–Aldrich Corp. St. Louis, MO, USA). In week 10, the selective p38 MAPK inhibitor,

SB 203580 hydrochloride (50 lg/kg) (Tocris Bioscience, R&D Systems, Inc., Minneapolis, MN, USA), was given prior to behavioral testing. Both drugs were dissolved in normal saline and given by intraperitoneal (i.p.) injection. Normal saline served as the vehicle control.

Mouse serum cytokine/chemokine protein profiling array

Mice were euthanized at 10 weeks after anesthesia with isoflurane. Blood (0.7–1 ml) was immediately drawn from the heart and placed into two serum separator microtainers with clot activator (30 min, R.T.) (BD, Franklin Lakes, NJ, USA). Samples were centrifuged (5000 rpm, 5 min) to collect sera prior to storage (80 °C) and analysis. Forty cytokines/chemokine proteins were analyzed in serum samples (100 ll) using the mouse cytokine Protein Proteomic Profiler™ Array kit (Mouse Cytokine Array Panel A, ARY006, R&D Systems, Minneapolis, MN, USA) according to the manufacturer's instructions. The resulting pixel densities of the protein immune-blot dots were quantified with image J (NIH). Two measurements from each sample were obtained and the pair of duplicate spots averaged. Only 39 of the 40 protein blots could be analyzed in the assays due to overlap in one case. The cytokine/chemokine levels (pixel densities) were compared among the four experimental groups: TNFR1/2 KO mice with or without TIC injury, as well as matched WT mice with or without TIC injury. Experiments were repeated in three cohorts of mice with one mouse in each group. A clinical evaluation standard for analyzing cytokines in sera of patients with pancreatitis was adopted to evaluate the cytokine changes in serum of mice with different genotypes and injuries (Torres et al., 2014). The relative values and ratios for those proteins were considered major changes if they were 50% above (1.5, red) or below (0.5, blue) the ratio value of 1. Proteins with values between 0.5 and 1.5 were considered no change (green).

Spinal trigeminal nucleus microglial immunohistology

Mice were euthanized with isoflurane and transcardially perfused with heparinized saline followed by 4% ice-cold paraformaldehyde in 0.1 M phosphate buffer solution (PB, pH 7.4). After the fixative perfusion, the medulla was dissected and post fixed (4 h). The tissues were switched to 30% sucrose (0.1 M PB, 24 h) and then embedded into Cryo-O.C.T. Tissue-Tek compound (Life Technologies, Grand Island, NY, USA). The tissue block was sectioned (12 lm) with a cryostat and mounted onto gel-coated glass slides. Sections were washed with 0.1 M phosphate-buffered saline (PBS, pH 7.4) and blocked with 5% non-fat milk (30 min, RT). Sections were batch processed, incubated with mouse anti-OX42 (1:1000, Abcam, Cambridge, MA, USA) antibody at 4 °C overnight. Primary antibody omission as a negative control and staining for a different primary antibody as a positive control were performed in parallel with the immunohistological study. Sections were incubated with secondary antibody, Alexa Fluor 488 goat anti-mouse antibody (1:1000, 1 h, Invitrogen, Grand Island, NY, USA). The slides were coverslipped with glycerol-based mount media (Vector Laboratories, Burlingame, CA, USA). Photos were captured in 20 magnification using a Nikon E1000 microscope (Nikon Instruments, Inc., Melville, NY, USA) equipped with the MetaVue 6.1 program (Molecular Devices, Downingtown, PA, USA). Microglial cells in the spinal trigeminal nucleus were counted with the assistance of MetaMorph offline software. Threshold was set on the digital images according to the background density in ipsilateral

tissue from the sham mice. This level was used throughout to assess the number of positive cells in other groups. The number of cells was averaged on both sides in five sections from each animal (n = 3 animals per group).

Statistical analysis

Data were analyzed with Prism 6 software (Graph Pad Software, Inc., La Jolla, CA, USA) and all the data were presented as mean ± SE. The head withdrawal threshold data were analyzed with a two-way analysis of variance (ANOVA) with Bonferroni multiple comparison tests for comparisons of each time point with their own baseline. Between- and within-groups comparisons were analyzed with repeated measures a one-way ANOVA with Geisser–Greenhouse's correction test. Cytokine profile data were analyzed with two-tailed t-test. A p value of ≤0.05 was considered significant.

RESULTS

Mechanical allodynia on bilateral whisker pads of TNFR1/2 KO mice after TIC injury

Mechanical threshold was tested with von Frey filament stimulation on both whisker pads on days 3 and 7 in the first week and once a week thereafter for a period of 10 weeks (70 days) (Fig. 1A). The behavioral responses were compared between and within the two groups over time for 10 weeks (Fig. 1A, B). There was no difference in the baseline responses between groups or side to side. The mechanical thresholds for the TNFR1/2 KO mice were variable for three weeks after sham surgery on both sides of the whisker pads, then they recovered and were not significantly different from their baseline. Although a significant decrease from baseline in week 3 could be detected when compared to baseline, there was no difference between ipsilateral and contralateral whisker pads in the TNFR1/2 KO sham mice overall (Fig. 1A).

On the ipsilateral whisker pad, the TNFR1/2 KO and WT mice with TIC injury exhibited mechanical allodynia 3 days after TIC injury compared to baseline (0.17 ± 0.05 g vs. 3.45 ± 0.00 g for TNFR1/2 KO $n = 5$; and 0.14 ± 0.04 vs. 3.47 ± 0.00 for WT $n = 6$; two-way ANOVA, Bonferroni multiple comparisons test, $F(3, 216) = 102.3$; $p < 0.001$, Fig. 1A, B). The mechanical allodynia on the ipsilateral whisker pad persisted through the entire experimental duration. In fact, in week 10, responses were 0.16 ± 0.05 g (TNFR1/2 KO TIC) vs. 3.17 ± 0.3 g (TNFR1/2 KO sham) and 0.27 ± 0.03 g (WT TIC) vs. 2.9±0.57 g (WT sham). In the overall analysis for TNFR1/2 KO mice, the ipsilateral mechanical thresholds were significantly decreased in TIC injury group compared to the sham group (repeated measures one-way ANOVA with Geiss er–Greenhouse's correction test, F (1, 11) = 57.11, $p < 0.001$) (Fig. 1A). The contralateral mechanical thresholds were significantly decreased in TIC injury group compared to the sham group (repeated measures one-way ANOVA with Geisser–Greenhouse's correction test, $F(1, 11) = 43.22$, $p < 0.001$) (Fig. 1A). The ipsilateral 50% mechanical thresholds were significantly decreased in WT TIC injury group compared to WT sham group (repeated measures one-way ANOVA with Geisser–Greenhouse's correction test, $F(1, 11) = 68.66$, $p < 0.001$). No statistically significant difference was detected between the TIC and sham WT mice for contralateral whisker pads (TIC: 3.03 ± 0.36 g vs. sham: 3.47 ± 0.00 g, $p > 0.05$).

On the contralateral whisker pads, mechanical allodynia progressively developed only in TNFR1/2 KO mice beginning in the third week after TIC injury [0.64 ± 0.21 g vs. 3.13 ± 0.57 g baseline, a two-way ANOVA, Bonferroni multiple comparisons test $F(3, 216) = 102.3$, $p < 0.001$]. No statistically significant difference was detected between the ipsilateral and contralateral whisker pads (TNFR KO TIC, $p > 0.05$, Fig. 1A, B). The mechanical threshold on contralateral whisker pad of TNFR1/2 KO mice with TIC injury also showed a statistically significant difference from that of WT mice with TIC injury starting from the third post injury week onward. A repeated measures one-way ANOVA analysis with Geisser–Greenhouse's correction test demonstrated a statistically significant overall difference [$F(1, 11) = 46.80$, $p < 0.001$] (Fig. 1B). A statistically significant difference was detected between the ipsilateral and contralateral whisker pads of WT mice with TIC [$F(1, 11) = 126.9$, $p < 0.001$] (Fig. 1B).

Serum cytokine/chemokine proteomic profile for TNFR1/2 KO and WT mice alterations with or without TIC injury (10-week)

Proteomic profiling determined the relative expression levels of 40 mouse cytokine/chemokine proteins in sera at the 10-week time point for the four groups of mice: Control WT, WT with TIC, Control TNFR1/2 KO and TNFR1/2 KO with TIC. The cytokine/chemokine data are presented with color coding in Tables 1–3. The relative values and ratios for those proteins were considered major changes if they were 50% above (1.5, red) or below (0.5, blue) the ratio of 1. Proteins with values between 0.5 and 1.5 were considered no change (green). Table 1 lists all the individual cytokine/chemokine values for the TNFR1/2 KO mice with TIC injury, for the TNFR1/2 KO control mice without TIC injury, as well as for the KO TIC/KO Control ratios. Table 2 lists the individual cytokine/chemokine values for WT mice with TIC injury, the WT control mice without TIC injury, as well as the WT TIC/WT Control ratios for the cytokines. Table 3 provides the individual serum cytokine/chemokines for both WT and TNFR1/2 KO mice after TIC injury, as well as the KO TIC/WT TIC cytokine ratios. The summary pie charts illustrate the percent change in the cytokines. Both the tables and the pie charts use the same color-coding scheme for proteins that were up-regulated (red), down-regulated (blue), or had no change (green), in the on-line version.

TNFR1/2 KO mice with and without TIC injury.—Table 1 shows individual and ratio data for TNFR1/2 KO mice with and without TIC injury. A total of 10 (26%) cytokines/chemokines were up-regulated in TNFR1/2 KO mice with TIC injury compared to TNFR1/2 controls. The up-regulated proteins included chemokine (C-C motif) ligand 4/macrophage inflammatory protein-1β(CCL4/MIP-1β), Eotoxin, CXCL12, colony stimulating factors granulocyte colony-stimulating factor (G-CSF), granulocyte–macrophage colony-stimulating factor (GMCSF), and inflammatory cytokines interleukin-1alpha (IL-1a) and interleukin-23 (IL-23). Seventy-four percent of the cytokines tested were unchanged. No down-regulated cytokines/chemokines were detected comparing TNFR1/2 KO mice 10 weeks following TIC injury to TNFR1/2 control mice. The pie chart summarizes the change in cytokine/chemokines in TNFR1/2 KO mice after TIC injury as a percentage of the total number of cytokines measured.

WT mice with and without TIC injury.—Table 2 shows individual and ratio data for WT mice with and without TIC injury. Only three cytokines/chemokines were up-regulated (8%) in WT animals after TIC injury. Of interest, B lymphocyte chemoattractant (CXCL-13) was up-regulated in WT mice with TIC injury similar to the TNFR1/2 KO mice. However, TREM-1 up-regulation was specific to the WT mice with TIC injury. Most intriguing, CCL3/MIPα which was significantly up-regulated in dysregulated TNFR1/2 KO mice, was actually down-regulated in WT mice after TIC injury. In WT mice, six different cytokines (15%) were down-regulated 10 weeks post TIC injury, and 77% were unchanged.

Comparison of TNFR1/2 KO and WT mice with TIC injury.—In Table 3, the cytokine profile of TNFR1/2 KO with TIC injury compared to WT mice with TIC injury indicated that 38% were up-regulated, 3% were down-regulated, and 59% were not different 10 weeks after nerve injury. Representative proteomic profiler arrays (A) are shown below the table with an arrow indicating the duplicate blots for TNFα in the serum of one TNFR1/2 KO mouse with TIC injury. Two representative cytokine proteomic profiler arrays are shown for TNFR1/2 KO with TIC (left) and for WT mice with TIC (right) for comparison. The pie chart (B) shows the summary of the percent changes in the number of serum cytokines/chemokines for the KO/WT mice with TIC injury. Another comparison between TNFR1/2 KO and WT mice without injury showed that CXCL12 was upregulated (1565 ± 410 vs. 2365 ± 442) and CCL11 was downregulated (1561 ± 112 vs. 860 ± 156) in TNFR1/2 KO mice.

Bilateral microglial activation in trigeminal nucleus of TNFR1/2 KO mice with TIC injury

Medullary brainstem sections were immunostained with anti-OX42 antibody to identify activated microglia in the spinal trigeminal nucleus (Fig. 2). Higher OX42 immunoreactivity was detected in both the ipsi- and contralateral spinal trigeminal nucleus in TNFR1/2 KO mice with TIC (Fig. 2A, B) than in WT mice with TIC injury (Fig. 2C, D). The basal level of OX42 in the WT (Fig. 2E) and TNFR1/2 KO sham groups (not shown) as barely detectable. An increase in OX42 immuno-reactivity indicates that chromic gut suture induced infraorbital nerve activation triggers microglial activation in the trigeminal nucleus. The bar graph (Fig. 2F) indicates the statistically significant increases of OX42-positive cells in trigeminal nucleus bilaterally in TNFR1/2 KO mice compared to the WT surgical sham mice both ipsilaterally as well as contralaterally (TNFR1/2 KO TIC, WT TIC vs. WT sham; *ipsi $p < 0.05$; **contra $p < 0.01$; $n = 3$/group) with a non-parametric one-way ANOVA test. The results for bilateral spinal trigeminal nucleus microglial activation after TIC injury in mice with disrupted TNFR1/2 are congruent with the bilateral whisker pad hypersensitivity following TIC injury.

Alleviation of bilateral orofacial hypersensitivity in TNFR1/2 KO mice by inhibition of microglia and the p38 MAP kinase pathway

With the speculation that microglial activation was contributing to the bilateral orofacial hypersensitivity, the effect of microglial activation inhibitor, minocycline, was tested for its efficacy in reducing whisker pad mechanical allodynia in TNFR1/2 KO mice with TIC injury in week 9. Bilateral behavioral changes were monitored for 1 h after minocycline administration (30 mg/kg, i.p.). Data showed that minocycline provided brief alleviation of

the bilateral whisker pad mechanical allodynia. The peak effect was at 30 min (ipsilateral: 1.29 ± 0.00 g vs. 0.19 ± 0.05 g, $n = 5$, $p < 0.001$; contralateral: 1.29 ± 0.00 g vs. 0.64 ± 0.21 g), and the analgesic effect subsided at 1 h (Fig. 3A).

SB203580 is a specific inhibitor of p38 MAP kinase activity. In week 10 after TIC injury, mechanical sensitivity was tested before and 0.5, 1, 3, 6 h after SB203580 (50 μg/kg, i.p.) administration in TNFR1/2 KO mice. In TNFR1/2 KO mice, the mechanical hypersensitivity of the ipsilateral side was significantly reduced 1 h after SB203580 administration (3.04 ± 0.49 vs. 0.32 ± 0.07 g, $n = 5$, $p < 0.01$) and was alleviated at 3 h after (Fig. 3B). The effect of SB203580 was also noticeable on the contralateral side of TNFR1/2 KO mice although the differences were not statistically significant. The mechanical threshold was elevated beginning at 0.5 h and did not return to the pre-drug level even at the 6-h time point. The SB203580 reduced whisker pad mechanical hypersensitivity bilaterally in TNFR1/2 KO mice with TIC injury. The saline injected as vehicle control had no effect (data not shown). The OX42 immunofluorescence was not examined after pharmacological treatment with minocycline or p38 inhibitor. The transient analgesic effect of these drugs was not expected to cause central morphological changes with a single dose.

DISCUSSION

The results of this study reflect behavioral changes and dysregulation of cytokines in TNFR1/2 KO mice after the TIC insult. Pain-related behavior was observed bilaterally and was paralleled by increases in both ipsilateral and contralateral microglial activation. Both hypersensitivity and microglial activation were unilateral in WT mice. Serum cytokine increase is one of contributors to contralateral whisker pad hypersensitivity and microglial activation in TNFR1/2 KO mice in the study.

Proteome profile alteration

The intensities of the proteome profile dot blots indicated levels of immune responsiveness in the mouse sera. Up to 38% of the cytokines/chemokines measured were increased in serum when considering the TNFR1/2 KO/WT ratios after TIC injury, with statistically significant increases for TNFα and IL-1α. TNFα can be released from affected peripheral nerves, dorsal root ganglia and central nervous tissue after nerve injury (Wagner and Myers, 1996; Marchand et al., 2005), potentially increasing CSF and serum levels (Ren et al., 2011), in addition to the systemic immune response due to the injury itself. TNFα is also measureable in both the CSF and serum in a clinical study of painful polyneuropathy (Ludwig et al., 2008). Blood samples from patients with different types of neuropathies have been tested for cytokine changes including those with painful, painless and control conditions (Uceyler et al., 2007). In patients with painful neuropathies, TNF mRNA was shown to be increased with levels varying depending on the type of neuropathy. It has been shown that TNF activates peripheral nerves in chronic constriction injury model in rats (Sommer and Schafers, 1998; Schafers et al., 2003) and maintains chronic neuropathic pain (Covey et al., 2002; Kleinschnitz et al., 2004; Ohtori et al., 2004).

It was reported that circulating TNFα is dramatically elevated in TNFR2 KO mice (Peschon et al., 1998). Previously, the question has arisen as to how excess TNFα can execute a

physiological role in the absence of its receptors. Structure and functional study reported the ability of three TNF molecules to form a transmembrane trimer with a central pore-like region (Kagan et al., 1992). The TNFα trimer forms a low pH-dependent, voltage-dependent, ion-permeable channel which increases the sodium permeability of inflammatory cells. The remarkable structure is similar to the “jelly-roll” motif structure characteristic of viral coat proteins on cellular membranes (Jones et al., 1989). This mechanism was later dismissed with findings that the TNF trimer is tethered to the receptor and that only after interaction with the receptor will it exert its effects (van der Goot et al., 1999; Uceyler et al., 2009). Transmembrane TNFα over-expression is reported in TNFR1/2 KO mice using an inflammatory arthritis model (Edwards et al., 2006). Other *in vitro* and *in vivo* studies also demonstrate that transmembrane TNFα contributes to microglial activation in neuropathic pain caused by spinal nerve ligation or partial spinal cord injury (Peng et al., 2006; Hao et al., 2007; Zhou et al., 2010).

The present study provides the cytokine proteome profile after the TIC injury that is potentially prolonging the nociceptive response since in their absence or dysregulated state the TNFα receptors cannot autoregulate TNFα levels. Data showed 26% of cytokines assayed were up-regulated in TNFR1/2 KO at 10 weeks compared to only 8% up-regulated in WT mice after TIC injury. This clearly emphasizes the impact of other serological inflammatory mediator changes for inducing bilateral microglial activation and mechanical allodynia. The increase in multiple cytokines also implies that TNFα is not the only mechanism responsible for the bilateral hypersensitivity observed in the TNFR1/2 KO mice with TIC injury.

The present study confirmed serum TNFα was increased in the mice with the dual TNFR1 and TNFR2 deficiency. In most biological processes, multiple cytokines operate in large networks and TNFα is an important factor initiating a cascade of cytokine activation. Absence of TNFRs contributed to the lack of feedback control for TNFα, however, many other cytokine increases were likely responsible for the continuing hypersensitivity in the present study including CCl4/MIP1β, IL-1α, GM-CSF, and IL-23, in particular.

Cytokines prolonging bilateral mechanical hypersensitivity in the absence of TNFR1/R2

Serum level alterations of various other inflammatory cytokines/chemokines are known to impact pain-related behaviors. Several cytokines have been shown to be involved in debilitating orofacial diseases at either nerve trauma sites or the relevant adjacent tissue. Although different inflammatory mediators are increased in trigeminal ganglion, inflammatory mediators increase more abundantly in the TMJ after CFA induced injury (Carleson et al., 1997; Spears et al., 2005). While serum cytokines can be measured, changes in cytokines are not always evident even in inflammatory conditions. For example, only elevation of serotonin was reported in serum of rheumatoid arthritis patients with TMJ pain among several inflammatory mediator candidates (Alstergren et al., 1999). However, many reports have appeared for increased somatic nociceptive responses attributed to IL-1α through increased prostaglandin E2 levels, although reports for cytokine involvement in trigeminal pain has been limited thus far to TMJ models. IL-1α and CCl4/MIP1β are reportedly present in synovial fluid of 80% and 68% patients with TMJ pain, respectively

(Matsumoto et al., 2006). MIP-1β, a regulator of neuronal glial interactions, has been shown to be increased acutely for 1–3 days in the injury site with the sciatic nerve injury model in mice (Saika et al., 2012). Serum levels of IL-23/IL-17 are reportedly elevated in periodontitis patients (Qi et al., 2013). IL-23 was the only cytokine reportedly above the detectable limit in human blood of patients with neuropathic pain in a report by Luchting et al. (2015). GMCSF is increased in T lymphocytes after L5 nerve transection in mice (Draleau et al., 2014). Thus, while few reports have appeared thus far, circulating levels of these cytokines/chemokines have begun to be linked to nociception.

Comparison between WT and KO uninjured mice showed CXCL12 was upregulated and CCL12 down-regulated in the TNFR1/2 KO mice. CXCL12 release could be induced in addition to dysregulated TNFα. We speculate that high concentration of CXCL12 inhibits CCL11 which belongs to the same chemokine family with CXCL12. Compensation may be involved in constitutive release in TNFR1/2 KO mice and cytokine changes exaggerated after TIC injury. Increased levels of CXCL12 could also be contributing to bilateral hypersensitivity in the chronic model although levels in the naı¨ve mice are not significantly different from baseline. Sciatic nerve hypersensitivity has been shown to be driven by CXCL1 speculated to be induced by TNFα and released from spinal astrocytes (Zhang et al., 2013).

Bilateral mechanical allodynia and microglial activation

In rats with WT, TNFR1 and TNFR2 KO genotypes, decreased unilateral mechanical thresholds have been reported after chronic constrictive injury of the sciatic nerve, although in other studies TNFR1 mice were less affected and the mechanical allodynia was partially reversed over time (Vogel et al., 2006). In the present study, the delayed, moderate mechanical allodynia also developed on the contralateral whisker pad in the TNFR1/2 KO mice. Bilateral orofacial hypersensitivity has been related to the brain stem medullary microglial activity increase in both animal and clinical studies. Spinal neurons are hyper-excitable when microglia are activated which accounts for bilateral allodynia reported in a model of unilateral focal burn injury in rats (Chang et al., 2010). Microglial cells primed by high levels of TNFα respond readily after injury, and thus microglial activation is reported to be causative in the central sensitization induced hypersensitivity after head and neck injury (Curatolo et al., 2001; Hubbard and Winkelstein, 2005). In the brain, however, TNFα can elicit either exacerbating or protective effects by activated signaling pathways that involve either microglial activation or increased oxidative stress, respectively (Sriram et al., 2006). This was demonstrated to be dependent on the specific brain region involved. Deficiency of TNF receptors was protective in mice injected with neurotoxic 1-methyl-4-phenyl-1,2,3,6-tetrahydropyridine to induce brain injury in TNFR1/2 KO mice, however, the deficiency had the opposite effect increasing damage in the hippocampus in the same mouse model (Sriram et al., 2006). TNFα provided neuroprotective effects in focal cerebral ischemia and epileptic seizure brain injury models primarily through an anti-oxidative pathway (Bruce et al., 1996). The TNFα overexpression developing in TNFR1/2 KO mice in an inflammatory arthritis model was accompanied by tissue swelling and bone deformities (Edwards et al., 2006).

In the present study, the side-to-side difference in the time course for development of whisker pad mechanical allodynia and the bilateral trigeminal nucleus microglial activation suggests sequential central mechanisms are invoked. The peripheral nerve injury initiates microglial activation on the ipsilateral side, while the microglial activation on the contralateral side was likely primed by TNFα as well as other circulating and local cytokines, such as IL-1α released in the TNFR1/2 KO mice. The result is hypersensitivity on the contralateral side. Both *in vitro* and *in vivo* studies have demonstrated that transmembrane TNFα as one of the cytokines contributing to microglial activation in neuropathic pain models induced by spinal nerve ligation or partial spinal cord injury (Peng et al., 2006; Hao et al., 2007; Zhou et al., 2010). It is reported that calcitonin gene-related peptide (CGRP) appears in the contralateral trigeminal ganglia in response to unilateral ligature-induced periodontitis after day 10 (Gaspersic et al., 2008). Similar to mechanisms proposed in that study, the contralateral microglial activation in the present study is likely mediated by crosstalk through the transmedian neurological pathways crossing in the trigeminal nuclear complex since microglia have CGRP receptors (Pfaller and Arvidsson, 1988; Edvinsson et al., 1989). We have observed inflammatory cells in the dissected nerve near the TIC insult at 10 weeks (Ma et al., 2012). The systemic inflammatory reaction to an initial injury and activation of the so called “neuro-immune axis” is modulated by the nucleus solitarius receiving vagal innervation (dorsal vagal complex) (Watkins et al., 1995; Tracey, 2002). The disrupted cytokine signaling in the TNFR1/2 KO mice likely affects the neuroimmune axis and the altered proteome profile. Alternatively, the nerve injury induced neurogenic excitation itself may invoke the neuroimmune axis in the TNFR1/2 KO, in addition to the prolonged hypersensitivity and proteome profile alteration. This suggests that similar genetic or epigenetic alterations can lead to chronic neuropathic pain in patients.

Block of microglial activation reduces mechanical allodynia

In the present study, both the microglial and the p38 MAPK inhibitors provided brief bilateral decrease in whisker pad hypersensitivity in TNFR1/2 KO mice with TIC injury after single dose injection. This suggests that longer term treatments with these inhibitors might be used clinically since they cross the blood–brain barrier. Minocycline used in our previous TIC model study in WT mice determined that microglial activation contributes to the hypersensitivity (Ma et al., 2012). The p38 inhibitor also completely blocked the mechanical allodynia at 1 h. These data for trigeminal nerve injury supports many other studies that report microglial activation is causal in the development of mechanical allodynia. For example, in a similar study Chang et al. discussed minocycline’s impact on microglial accumulation and found that long term systemic treatment with minocycline could significantly decrease microglial activation (Chang and Waxman, 2010). They reported CGRP and SP were normalized at 10 weeks, but glial activation was significantly increased. Long term treatment with minocycline reduced mechanical allodynia in their study for several weeks. The transient effect of minocycline was also evident in sciatic nerve chronic constrictive injury rats after injection into the posterolateral nucleus of the thalamus (LeBlanc et al., 2011). Systemic application of minocycline acutely attenuated acetic acid induced visceral nociceptive behavior and decreased c-Fos (Cho et al., 2012). There could be other minocycline effects on signaling and/or reduction in numbers of activated microglia. Minocycline inhibition of synaptic currents in the substantia gelatinosa is reported for

formalin-induced inflamma-tory pain and the ERK inhibitor suppression of the acetic acid-induced visceral pain may bridge the minocycline effect in nociception (Cho et al., 2006, 2012). Thus, the mechanisms for microglial activation may involve p38 mediation after TNF priming on the contralateral side of the brain stem (Schafers et al., 2003). Considering peripheral, central, and systemic methods of p38 inhibitor delivery, all of them attenuate capsaicin-induced hind paw hyperalgesia (Sweitzer et al., 2004b). Our data find in agreement with these studies that increase in mechanical threshold was evident bilaterally on the whisker pad following single p38 inhibitor systemic administration. The acute effect of p38 was also reported in diabetes-induced neuropathic pain when delivered intraperitoneally (Sweitzer et al., 2004a). However, p38 may participate in contralateral signaling transduction either upstream of microglial activation following cytokine priming or downstream after microglial activation. Our result finding suppression of mechanical allodynia bilaterally with p38 MAPK inhibition in TNFR1/2 KO mice with TIC-induced nerve injury is supportive of downstream pathway signaling after microglial activation as a causal mechanism (Hua et al., 2005). While transitory analgesic effects were shown with these two drugs, this would not likely change microglial morphology of trigeminal nucleus in such a brief period. It is suggestive, however, that continued study with chronic dosing would be beneficial for reducing microglial activation as well as hypersensitivity.

CONCLUSION

The current study demonstrates continuous and persisting bilateral orofacial pain-like behaviors in TNFR1/2 KO mice after TIC of the infraorbital nerve. The cytokine profile indicated increases in CCl4/MIP1β, IL-1α, GM-CSF, and IL-23, in particular, accompany the mechanical hypersensitivity. Dysregulation of numerous serum cytokines and bilateral microglial activation triggered in the mice lacking both TNFα receptors after the trigeminal nerve injury indicates involvement of both humoral and neurogenic influences. These conditions lead to widespread, persisting systemic immune responses that account for the bilateral orofacial mechanical allodynia in the chronic trigeminal neuropathic pain model.

Acknowledgments—

The investigation was supported from internal institutional sources from the University of Kentucky President’s Research Professorship Fund (KNW) and College of Medicine Dean’s Start-up Fund (KNW).

Abbreviations:

ANOVA	analysis of variance
CFA	complete Freund’s adjuvant
CGRP	calcitonin gene-related peptide
CSF	cerebrospinal fluid
ERK	extracellular-signal-regulated kinase
GM-CSF	granulocyte–macrophage colony-stimulating factor

IL-1α	interleukin-1alpha
IL-5	interleukin-5
IL-23	interleukin-23
KO	knockout
MIP-1β	chemokine (C-C motif) ligand 4/macrophage inflammatory protein-1β
PB	phosphate buffer
TACE	tumor necrosis factor converting enzyme
TIC	trigeminal inflammatory compression
TMJ	temporomandibular joint
TNFα	tumor necrosis factor alpha
TNFR	tumor necrosis factor alpha receptor
WT	wild-type

REFERENCES

Alstergren P, Ernberg M, Kopp S, Lundeberg T, Theodorsson E (1999) TMJ pain in relation to circulating neuropeptide Y, serotonin, and interleukin-1 beta in rheumatoid arthritis. J. Orofac Pain 13:49–55. [PubMed: 10425968]

An JX, He Y, Qian XY, Wu JP, Xie YK, Guo QL, Williams JP, Cope DK (2011) A new animal model of trigeminal neuralgia produced by administration of cobra venom to the infraorbital nerve in the rat. Anesth Analg 113:652–656. [PubMed: 21778333]

Andrade P, Visser-Vandewalle V, Hoffmann C, Steinbusch HW, Daemen MA, Hoogland G (2011) Role of TNF-alpha during central sensitization in preclinical studies. Neurol Sci 32:757–771. [PubMed: 21559854]

Becerra L, Morris S, Bazes S, Gostic R, Sherman S, Gostic J, Pendse G, Moulton E, Scrivani S, Keith D, Chizh B, Borsook D (2006) Trigeminal neuropathic pain alters responses in CNS circuits to mechanical (brush) and thermal (cold and heat) stimuli. J Neurosci 26:10646–10657. [PubMed: 17050704]

Benoliel R, Wilensky A, Tal M, Eliav E (2002) Application of a proinflammatory agent to the orbital portion of the rat infraorbital nerve induces changes indicative of ongoing trigeminal pain. Pain 99:567–578. [PubMed: 12406533]

Bruce AJ, Boling W, Kindy MS, Peschon J, Kraemer PJ, Carpenter MK, Holtsberg FW, Mattson MP (1996) Altered neuronal and microglial responses to excitotoxic and ischemic brain injury in mice lacking TNF receptors. Nat Med 2:788–794. [PubMed: 8673925]

Carleson J, Bileviciute I, Theodorsson E, Appelgren B, Appelgren A, Yousef N, Kopp S, Lundeberg T (1997) Effects of adjuvant on neuropeptide-like immunoreactivity in the temporomandibular joint and trigeminal ganglia. J Orofac Pain 11:195–199. [PubMed: 9610308]

Chang YW, Waxman SG (2010) Minocycline attenuates mechanical allodynia and central sensitization following peripheral second-degree burn injury. J Pain 11:1146–1154. [PubMed: 20418178]

Chang YW, Tan A, Saab C, Waxman S (2010) Unilateral focal burn injury is followed by long-lasting bilateral allodynia and neuronal hyperexcitability in spinal cord dorsal horn. J Pain 11:119–130. [PubMed: 19744891]

Chaplan SR, Bach FW, Pogrel JW, Chung JM, Yaksh TL (1994) Quantitative assessment of tactile allodynia in the rat paw. J Neurosci Methods 53:55–63. [PubMed: 7990513]

Cho IH, Chung YM, Park CK, Park SH, Lee H, Kim D, Piao ZG, Choi SY, Lee SJ, Park K, Kim JS, Jung SJ, Oh SB (2006) Systemic administration of minocycline inhibits formalin-induced inflammatory pain in rat. Brain Res 1072:208–214. [PubMed: 16427032]

Cho IH, Lee MJ, Jang M, Gwak NG, Lee KY, Jung HS (2012) Minocycline markedly reduces acute visceral nociception via inhibiting neuronal ERK phosphorylation. Mol Pain 8:13. [PubMed: 22364340]

Covey WC, Ignatowski TA, Renauld AE, Knight PR, Nader ND, Spengler RN (2002) Expression of neuron-associated tumor necrosis factor alpha in the brain is increased during persistent pain. Reg Anesth Pain Med 27:357–366. [PubMed: 12132059]

Curatolo M, Petersen-Felix S, Arendt-Nielsen L, Giani C, Zbinden AM, Radanov BP (2001) Central hypersensitivity in chronic pain after whiplash injury. Clin J Pain 17:306–315. [PubMed: 11783810]

Draleau K, Maddula S, Slaiby A, Nutile-McMenemy N, De Leo J, Cao L (2014) Phenotypic identification of spinal cord-infiltrating CD4 T lymphocytes in a murine model of neuropathic pain. J Pain Relief Suppl 3:003.

Edvinsson L, Hara H, Uddman R (1989) Retrograde tracing of nerve fibers to the rat middle cerebral artery with true blue: colocalization with different peptides. J Cereb Blood Flow Metab 9:212–218. [PubMed: 2466041]

Edwards CK, 3rd, Bendele AM, Reznikov LI, Fantuzzi G, Chlipala ES, Li L, Moldawer LL, Mountz JD, Li YY, Dinarello CA (2006) Soluble human p55 and p75 tumor necrosis factor receptors reverse spontaneous arthritis in transgenic mice expressing transmembrane tumor necrosis factor alpha. Arthritis Rheum 54:2872–2885. [PubMed: 16947419]

Empl M, Renaud S, Erne B, Fuhr P, Straube A, Schaeren-Wiemers N, Steck AJ (2001) TNF-alpha expression in painful and nonpainful neuropathies. Neurology 56:1371–1377. [PubMed: 11376190]

Fang C, Shi B, Pei YY, Hong MH, Wu J, Chen HZ (2006) In vivo tumor targeting of tumor necrosis factor-alpha-loaded stealth nanoparticles: effect of MePEG molecular weight and particle size. Eur J Pharm Sci 27:27–36. [PubMed: 16150582]

Gaspersic R, Kovacic U, Cor A, Skaleric U (2008) Unilateral ligature-induced periodontitis influences the expression of neuropeptides in the ipsilateral and contralateral trigeminal ganglion in rats. Arch Oral Biol 53:659–665. [PubMed: 18342833]

Gregersen R, Lambertsen K, Finsen B (2000) Microglia and macrophages are the major source of tumor necrosis factor in permanent middle cerebral artery occlusion in mice. J Cereb Blood Flow Metab 20:53–65. [PubMed: 10616793]

Hao S, Mata M, Glorioso JC, Fink DJ (2007) Gene transfer to interfere with TNFAlpha signaling in neuropathic pain. Gene Ther 14:1010–1016. [PubMed: 17443214]

Hide I, Tanaka M, Inoue A, Nakajima K, Kohsaka S, Inoue K, Nakata Y (2000) Extracellular ATP triggers tumor necrosis factor-alpha release from rat microglia. J Neurochem 75:965–972. [PubMed: 10936177]

Hua XY, Svensson CI, Matsui T, Fitzsimmons B, Yaksh TL, Webb M (2005) Intrathecal minocycline attenuates peripheral inflammation-induced hyperalgesia by inhibiting p38 MAPK in spinal microglia. Eur J Neurosci 22:2431–2440. [PubMed: 16307586]

Hubbard RD, Winkelstein BA (2005) Transient cervical nerve root compression in the rat induces bilateral forepaw allodynia and spinal glial activation: mechanical factors in painful neck injuries. Spine 30:1924–1932. [PubMed: 16135981]

Jones EY, Stuart DI, Walker NP (1989) Structure of tumour necrosis factor. Nature 338:225–228. [PubMed: 2922050]

Kagan BL, Baldwin RL, Munoz D, Wisnieski BJ (1992) Formation of ion-permeable channels by tumor necrosis factor-alpha. Science 255:1427–1430. [PubMed: 1371890]

Kawasaki Y, Zhang L, Cheng JK, Ji RR (2008) Cytokine mechanisms of central sensitization: distinct and overlapping role of interleukin-1beta, interleukin-6, and tumor necrosis factor-alpha in

regulating synaptic and neuronal activity in the superficial spinal cord. J Neurosci 28:5189–5194. [PubMed: 18480275]

Kleinschnitz C, Brinkhoff J, Zelenka M, Sommer C, Stoll G (2004) The extent of cytokine induction in peripheral nerve lesions depends on the mode of injury and NMDA receptor signaling. J Neuroimmunol 149:77–83. [PubMed: 15020067]

Koch A, Zacharowski K, Boehm O, Stevens M, Lipfert P, von Giesen HJ, Wolf A, Freynhagen R (2007) Nitric oxide and proinflammatory cytokines correlate with pain intensity in chronic pain patients. Inflamm Res 56:32–37. [PubMed: 17334668]

Kreutzberg GW (1996) Microglia: a sensor for pathological events in the CNS. Trends Neurosci 19:312–318. [PubMed: 8843599]

LeBlanc BW, Zerah ML, Kadasi LM, Chai N, Saab CY (2011) Minocycline injection in the ventral posterolateral thalamus reverses microglial reactivity and thermal hyperalgesia secondary to sciatic neuropathy. Neurosci Lett 498:138–142. [PubMed: 21571034]

Locksley RM, Killeen N, Lenardo MJ (2001) The TNF and TNF receptor superfamilies: integrating mammalian biology. Cell 104:487–501. [PubMed: 11239407]

Luchting B, Rachinger-Adam B, Heyn J, Hinske LC, Kreth S, Azad SC (2015) Anti-inflammatory T-cell shift in neuropathic pain. J Neuroinflamm 12:12.

Ludwig J, Binder A, Steinmann J, Wasner G, Baron R (2008) Cytokine expression in serum and cerebrospinal fluid in noninflammatory polyneuropathies. J Neurol Neurosurg Psychiatry 79:1268–1273. [PubMed: 18550631]

Ma F, Zhang L, Lyons D, Westlund KN (2012) Orofacial neuropathic pain mouse model induced by trigeminal inflammatory compression (TIC) of the infraorbital nerve. Mol Brain 5:44. [PubMed: 23270529]

Marchand F, Perretti M, McMahon SB (2005) Role of the immune system in chronic pain. Nat Rev Neurosci 6:521–532. [PubMed: 15995723]

Matsumoto K, Honda K, Ohshima M, Yamaguchi Y, Nakajima I, Micke P, Otsuka K (2006) Cytokine profile in synovial fluid from patients with internal derangement of the temporomandibular joint: a preliminary study. Dentomaxillofac Radiol 35:432–441. [PubMed: 17082335]

Ogawa N, Kawai H, Terashima T, Kojima H, Oka K, Chan L, Maegawa H (2014) Gene therapy for neuropathic pain by silencing of TNF-alpha expression with lentiviral vectors targeting the dorsal root ganglion in mice. PLoS ONE 9:e92073. [PubMed: 24642694]

Ohtori S, Takahashi K, Moriya H, Myers RR (2004) TNF-alpha and TNF-alpha receptor type 1 upregulation in glia and neurons after peripheral nerve injury: studies in murine DRG and spinal cord. Spine 29:1082–1088. [PubMed: 15131433]

Peng XM, Zhou ZG, Glorioso JC, Fink DJ, Mata M (2006) Tumor necrosis factor-alpha contributes to below-level neuropathic pain after spinal cord injury. Ann Neurol 59:843–851. [PubMed: 16634039]

Peschon JJ, Torrance DS, Stocking KL, Glaccum MB, Otten C, Willis CR, Charrier K, Morrissey PJ, Ware CB, Mohler KM (1998) TNF receptor-deficient mice reveal divergent roles for p55 and p75 in several models of inflammation. J Immunol 160:943–952. [PubMed: 9551933]

Pfaller K, Arvidsson J (1988) Central distribution of trigeminal and upper cervical primary afferents in the rat studied by anterograde transport of horseradish peroxidase conjugated to wheat germ agglutinin. J Comp Neurol 268:91–108. [PubMed: 3346387]

Qi Y, Feng W, Song A, Song H, Yan S, Sun Q, Yang P (2013) Role of serum IL-23/IL-17 axis in the relationship between periodontitis and coronary heart disease. Int J Periodontics Restorative Dent 33:185–191. [PubMed: 23484173]

Ren WJ, Liu Y, Zhou LJ, Li W, Zhong Y, Pang RP, Xin WJ, Wei XH, Wang J, Zhu HQ, Wu CY, Qin ZH, Liu G, Liu XG (2011) Peripheral nerve injury leads to working memory deficits and dysfunction of the hippocampus by upregulation of TNF-alpha in rodents.. Neuropsychopharmacology 36:979–992. [PubMed: 21289602]

Saika F, Kiguchi N, Kobayashi Y, Fukazawa Y, Kishioka S (2012) CC-chemokine ligand 4/macrophage inflammatory protein-1beta participates in the induction of neuropathic pain after peripheral nerve injury. Eur J Pain 16:1271–1280. [PubMed: 22528550]

Schafers M, Svensson CI, Sommer C, Sorkin LS (2003) Tumor necrosis factor-alpha induces mechanical allodynia after spinal nerve ligation by activation of p38 MAPK in primary sensory neurons. J Neurosci 23:2517–2521. [PubMed: 12684435]

Sommer C, Schafers M (1998) Painful mononeuropathy in C57BL/Wld mice with delayed wallerian degeneration: differential effects of cytokine production and nerve regeneration on thermal and mechanical hypersensitivity. Brain Res 784:154–162. [PubMed: 9518588]

Sommer C, Schmidt C, George A (1998) Hyperalgesia in experimental neuropathy is dependent on the TNF receptor 1. Exp Neurol 151:138–142. [PubMed: 9582261]

Sommer C, Lindenlaub T, Teuteberg P, Schafers M, Hartung T, Toyka KV (2001) Anti-TNF-neutralizing antibodies reduce pain-related behavior in two different mouse models of painful mononeuropathy. Brain Res 913:86–89. [PubMed: 11532251]

Sorkin LS, Doom CM (2000) Epineurial application of TNF elicits an acute mechanical hyperalgesia in the awake rat. J Peripher Nerv Syst 5:96–100. [PubMed: 10905468]

Spears R, Dees LA, Sapozhnikov M, Bellinger LL, Hutchins B (2005) Temporal changes in inflammatory mediator concentrations in an adjuvant model of temporomandibular joint inflammation. J Orofac Pain 19:34–40. [PubMed: 15779537]

Sriram K, Matheson JM, Benkovic SA, Miller DB, Luster MI, O'Callaghan JP (2006) Deficiency of TNF receptors suppresses microglial activation and alters the susceptibility of brain regions to MPTP-induced neurotoxicity: role of TNF-alpha. FASEB J 20:670–682. [PubMed: 16581975]

Stoll G, Jander S (1999) The role of microglia and macrophages in the pathophysiology of the CNS. Prog Neurobiol 58:233–247. [PubMed: 10341362]

Sweitzer SM, Medicherla S, Almirez R, Dugar S, Chakravarty S, Shumilla JA, Yeomans DC, Protter AA (2004a) Antinociceptive action of a p38alpha MAPK inhibitor, SD-282, in a diabetic neuropathy model. Pain 109:409–419. [PubMed: 15157702]

Sweitzer SM, Peters MC, Ma JY, Kerr I, Mangadu R, Chakravarty S, Dugar S, Medicherla S, Protter AA, Yeomans DC (2004b) Peripheral and central p38 MAPK mediates capsaicin-induced hyperalgesia. Pain 111:278–285. [PubMed: 15363871]

Thacker MA, Clark AK, Marchand F, McMahon SB (2007) Pathophysiology of peripheral neuropathic pain: immune cells and molecules. Anesth Analg 105:838–847. [PubMed: 17717248]

Torres C, Perales S, Alejandre MJ, Iglesias J, Palomino RJ, Martin M, Caba O, Prados JC, Aranega A, Delgado JR, Irigoyen A, Ortuno FM, Rojas I, Linares A (2014) Serum cytokine profile in patients with pancreatic cancer. Pancreas 43:1042–1049. [PubMed: 24979617]

Tracey KJ (2002) The inflammatory reflex. Nature 420:853–859. [PubMed: 12490958]

Uceyler N, Rogausch JP, Toyka KV, Sommer C (2007) Differential expression of cytokines in painful and painless neuropathies. Neurology 69:42–49. [PubMed: 17606879]

Uceyler N, Schafers M, Sommer C (2009) Mode of action of cytokines on nociceptive neurons. Exp Brain Res 196:67–78. [PubMed: 19290516]

van der Goot FG, Pugin J, Hribar M, Fransen L, Dunant Y, De Baetselier P, Bloc A, Lucas R (1999) Membrane interaction of TNF is not sufficient to trigger increase in membrane conductance in mammalian cells. FEBS Lett 460:107–111. [PubMed: 10571070]

Vogel C, Stallforth S, Sommer C (2006) Altered pain behavior and regeneration after nerve injury in TNF receptor deficient mice. J Peripher Nerv Syst 11:294–303. [PubMed: 17117937]

Wagner R, Myers RR (1996) Endoneurial injection of TNF-alpha produces neuropathic pain behaviors. NeuroReport 7:2897–2901. [PubMed: 9116205]

Watkins LR, Goehler LE, Relton JK, Tartaglia N, Silbert L, Martin D, Maier SF (1995) Blockade of interleukin-1 induced hyperthermia by subdiaphragmatic vagotomy: evidence for vagal mediation of immune-brain communication. Neurosci Lett 183:27–31. [PubMed: 7746479]

Westlund KN, Zhang L, Ma F, Oz HS (2012) Chronic inflammation and pain in a tumor necrosis factor receptor (TNFR) (p55/p75-/-) dual deficient murine model. Transl Res 160:84–94. [PubMed: 22687964]

Woolf CJ, Allchorne A, Safieh-Garabedian B, Poole S (1997) Cytokines, nerve growth factor and inflammatory hyperalgesia: the contribution of tumour necrosis factor alpha. Br J Pharmacol 121:417–424. [PubMed: 9179382]

Zhang L, Berta T, Xu ZZ, Liu T, Park JY, Ji RR (2011) TNF-alpha contributes to spinal cord synaptic plasticity and inflammatory pain: distinct role of TNF receptor subtypes 1 and 2. Pain 152:419–427. [PubMed: 21159431]

Zhang ZJ, Cao DL, Zhang X, Ji RR, Gao YJ (2013) Chemokine contribution to neuropathic pain: respective induction of CXCL1 and CXCR2 in spinal cord astrocytes and neurons. Pain 154:2185–2197. [PubMed: 23831863]

Zhou Z, Peng X, Hagshenas J, Insolera R, Fink DJ, Mata M (2010) A novel cell-cell signaling by microglial transmembrane TNFAlpha with implications for neuropathic pain. Pain 151:296–306. [PubMed: 20609516]

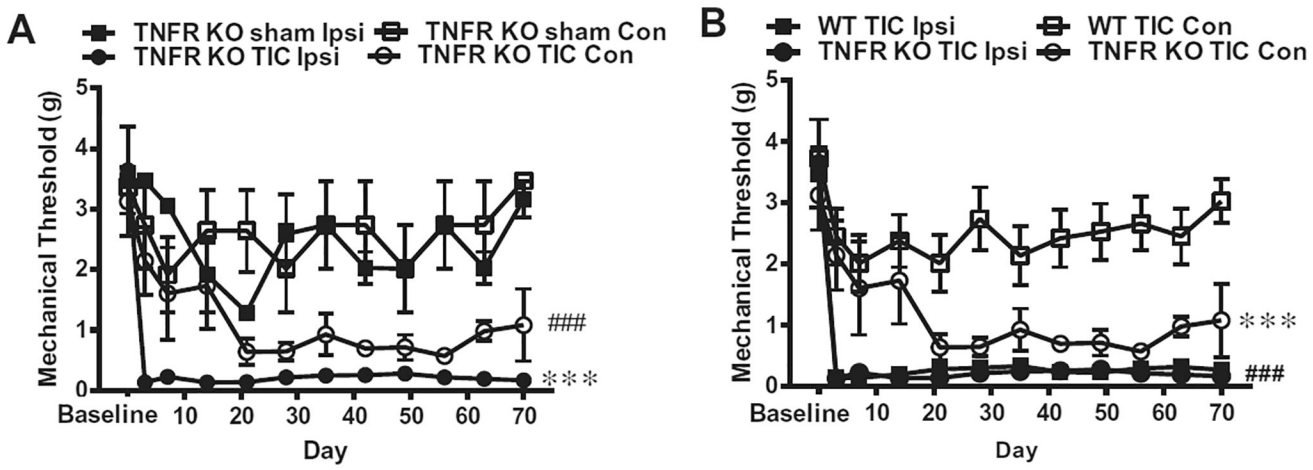

Fig. 1.

Bilateral mechanical allodynia of whisker pads in TNFR1/2 KO mice. (A) Mechanical allodynia is indicated by the decrease in the mechanical threshold (in grams force). TNFR1/2 KO mice had statistically significant decreases in mechanical threshold 3 days after TIC injury on the ipsilateral side (ipsi) that persisted through the end of the experiment. The decreased mechanical threshold on the contralateral side (Con) 3 weeks after TIC injury persisted through the remaining 8 weeks of the experiment ($n = 6$; ***$p < 0.001$ TNFR1/2 KO mice ipsilateral side vs. sham surgery; ###$p < 0.001$ TNFR1/2 KO mice contralateral side vs. sham surgery. $^{\S}p < 0.05$ TNFR1/2 KO sham vs baseline). (B) Mechanical threshold decreased on both ipsilateral and contralateral sides in mice with TIC injury ($n = 6$) but no difference was detected between the ipsilateral and contralateral sides. Mechanical threshold decreased on the ipsilateral side of WT mice with TIC injury ($n = 6$). There were significant differences between ipsilateral and contralateral side beginning 3 days after TIC injury that persisted for the entire experimental time course. A statistically significant difference was also found between the contralateral sides of WT and TNFR KO on post injury day 21 and thereafter. ($^{***}p < 0.001$ WT TIC contralateral side vs. TNFR1/2 KO TIC contralateral; $^{###}p < 0.001$ WT TIC ipsi vs. WT TIC contralateral).

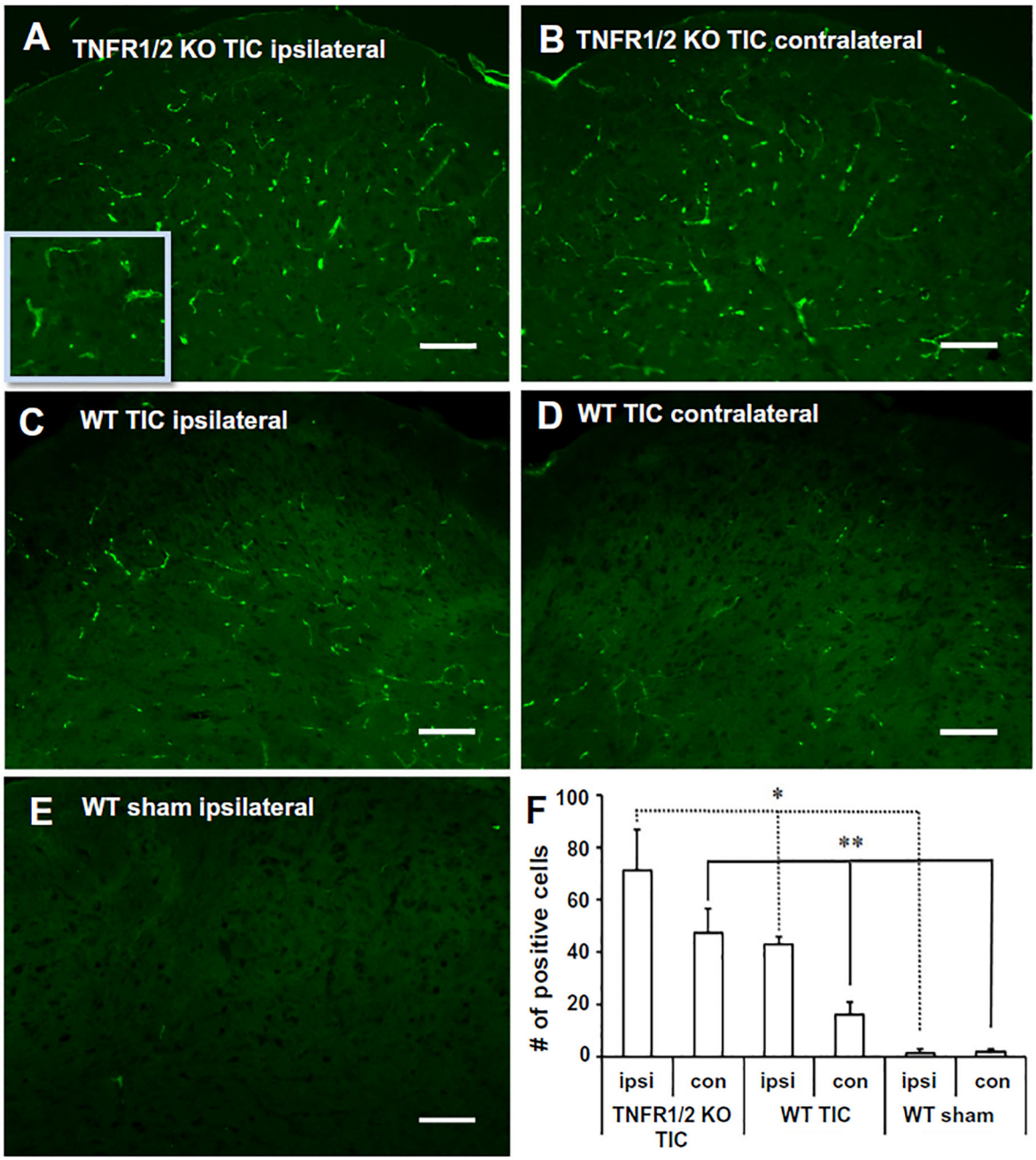

Fig. 2.

OX-42 immunohistology indicates microglial activation in spinal trigeminal nucleus. (A) Increased OX42 immunoreactivity was identified both ipsi- and (B) contralaterally in the spinal trigeminal nucleus of TNFR1/2 KO mice 10 weeks after TIC injury. (C) OX42-like immunoreactivity was evident in the ipsilateral spinal trigeminal nucleus, (D) but was minimal in the contralateral side of WT mice with TIC. (E) There was minimal OX-42 immunoreactivity detected in the brainstem spinal trigeminal nucleus of WT sham mice. (F) The bar graph illustrates the statistically significant increase of OX42 positive cells in trigeminal nucleus bilaterally in TNFR1/2 KO mice. (*$p < 0.05$ ipsilateral in TNFR1/2 KO

TIC, WT TIC and WT sham; $^{**}p < 0.01$ contralateral in TNFR1/2 KO TIC, WT TIC and WT sham, non-parametric one-way ANOVA) The inset in (A) provides better detail of the region above the calibration bar. Calibration bar: 100 μm.

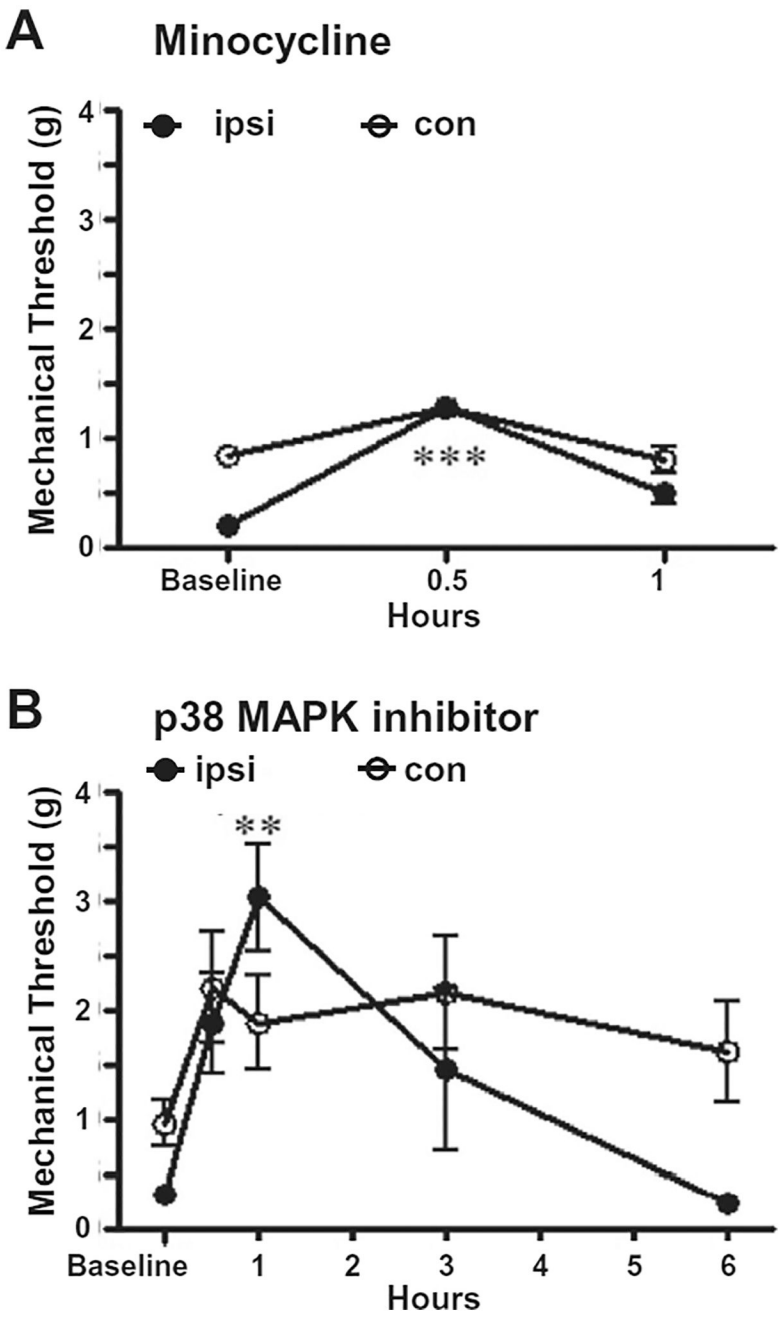

Fig. 3.

Microglial and p38 MAPK inhibitors reduced bilateral mechanical hypersensitivity in TIC injured TNFR1/2 KO mice. (A) Microglial activation inhibitor, minocycline, administered in week 9 provided brief alleviation of mechanical allodynia in TNFR1/2 KO mice. Behavioral improvement was best at 30 min after administration ($n = 6$; ***$p < 0.001$ vs. mechanical threshold at the zero time point before minocycline administration). (B) In week 10, the p38 MAPK inhibitor, SB203580, alleviated TIC injury induced mechanical allodynia bilaterally in TNFR1/2 KO beginning at 0.5 h, peaking at 1 h, and persisting for 3 h. The mechanical threshold of the contralateral whisker pad was elevated at 0.5 h and had not returned to

pretreatment levels at the 6-h time point ($n = 6$; $^{**}p < 0.01$ vs. mechanical threshold at the zero time point before drug treatment, one-way ANOVA).

Table 1.

TNFR1/2 KO mice with and without TIC injury

Protein	Abbreviation	*Gene*	Mean Pixel Density		Ratio
			Control	TIC	TIC/CON
B lymphocyte chemoattractant	BLC/CXCL13/BCA1	*CXCL13*	1152±276	2059±720	1.80
Cheraokine (C-C motif) ligand 2/monocyte ehemotaetic protein-1	CCL2(MCP-1)	*JE*	2683±576	3915±514	1.5
Chemokine (C-C motif) ligand 4/Macrophage inflammatory protein-1β	CCL4/MIP-1β	*CCL4*	812±242	2049±1144	2.5
Eotaxin/Chemokme (C-C motif) ligand 11	Eotaxin (CCL11)	*CCL11*	860±156	1590±885	1.85
Chemokine (C-C motif) ligand 12	CCL12/MCP-5	*CCL12*	1080±384	1811±873	1.68
Chemokine (C-C motif) ligand 17	CCL17/TARC	*CCL17*	1684±741	3670±1798	2.18
Granulocyte colony stimulating factor	G-CSF	*CSF3*	1503±289	2752±753	1.83
Granulocyte-macrophage colony-stimulating factor	GM-CSF	*CFS2*	1110±472	1833±997	1.65
Interleukin 1α	IL-1A	*IL1A*	3239±365	5017±680	1.54
Interleukin 23	IL-23	*IL-23*	1898±260	3647±1707	1.92
C5a anaphylatoxins/Complement component5	C5a	*C5*	5164±605	5345±271	1.04
Chemokine (C-C motif) ligand 1	I-309 (CCL1, TCA3)	*CCL1*	1114±179	1098±74	0.98
Chemokine (C-C motif) ligand 3/Macrophage inflammatory protein-1α	CCL3/MIP-1α	*CCL3*	696±201	438±104	0.63
Chemokine (C-C motif) ligand 5	CCL5/RANTES	*CCL5*	1450±106	1105±286	0.76
Chemokine (C-X-C motif) ligand 1/melanoma growth stimulating activity alpha	KC/CXCL1	*CXCL1*	3452±454	3332±495	0.96
Chemokine (C-X-C motif) ligand 2	MIP-2/CXCL2	*CXCL2*	1078±200	759±171	0.70
Chemokine (C-X-C motif) ligand 9/ Monokine induced by gamma interferon	CXCL9/MIG	*CXCL9*	1739±496	2172±568	1.25
Chemokine (C-X-C motif) ligand 10	CXCL10/IP-10/CRG-2	*CXCL10*	1404±277	1976±455	1.41
Chemokine (C-X-C motif) ligand 11	CXCL11/I-TAC	*CXCL11*	781±185	996±180	1.28
Chemokine (C-X-C motif) ligand 12	SDF-1/CXCL-12	*CXCL12*	2365±442	2758±650	1.17
Colony stimulating factor 1 (macrophage)	M-CSF	*CFS1*	3749±422	4661±578	1.24
Interferon gamma	IFN-γ	*IFNG*	4936±1074	4558±878	0.92
Interleukin 1β	IL-1β/IL-1F2	*IL1B*	1992±417	1976±676	0.99
Interleukin 2	IL-2	*IL-2*	2562±445	2848±661	1.11
Interleukin 3	IL-3	*IL-3*	2094±515	2826±738	1.35
Interleukin 4	IL-4	*IL-4*	3771±619	4469±1288	1.19

Protein	Abbreviation	*Gene*	Mean Pixel Density		Ratio
			Control	TIC	TIC/CON
Interleukin 5	IL-5	*IL-5*	1941±1067	1832±675	0.94
Interleukin 6	IL-6	*IL6*	1119±448	825±159	0.74
Interleukin 7	IL-7	*IL-7*	3716±948	5369±2271	1.44
Interleukin 10	IL-10	*IL-10*	1082±427	1482±828	1.37
Interleukin 12	IL-12/p70	*IL12A*	333±66	389±176	1.17
Interleukin 13	IL-13	*IL-13*	2866±200	3195±421	1.11
Interleukin 16	IL-16	*IL16*	3874±216	5747±846	1.48
Interleukin 17	IL-17	*IL-17*	2881±401	2905±826	1.00
Interleukin 27	IL-27	*IL27*	3175±695	2510±463	0.79
TIMP metallopeptidase inhibitor 1	TIMP-1	*TIMP1*	9263±1280	9845±399	1.06
Triggering receptor expressed on myeloid cells-1	TREM-1	*TREM1*	2746±887	3958±165	1.44
Tumor necrosis factor alpha	TNFα/TNFSF2	*TNF*	4241±984	5167±493	1.22

Summary of serum cytokine profile changes of TNFR1/2 mice w/wo TIC

Table 2.

Wild type mice with and without TIC injury

Protein	Abbreviation	*Gene*	Mean Pixel Density		Ratio
			WT	KO	KO/WT
B lymphocyte chemoattractant IL-1 receptor antagonist	BLC/BCA-1	*CXCL-13*	1275±227	2182±511	1.71
	IL-1ra/IL-1F3	*IL1RN*	2684±732	4443±1399	1.65
Triggering receptor expressed on myeloid cells-1	TREM-1	*TREM-1*	3135±555	5810±826	1.85
Chemokine (C-C motif) ligand 3/ Macrophage inflammatory protein-1α	CCL3/MIP-1α	*CCL3*	834±64	403±91	0.48
Chemokine (C-C motif) ligand 4/ Macrophage inflammatory protein-1β Chemokine (C-X-C motif) ligand 9/ Monokine induced by gamma interferon	CCL4/MIP-1β	*CCL4*	1092±526	513±175	0.47
	CXCL9/MIG	*CXCL9*	2243±517	1114±235	0.49
Interleukin 5	IL-5	*1L-S*	2285±1242	220±69	0.10
Interleukin 12	IL-12/p70	*IL-12A*	664±169	238±86	0.36
Interleukin 17	IL-17	*IL-17*	2926±505	1460±250	0.49
C5a anaphylatoxins/Complement components5a	C5a	*C5*	5526±199	5968±228	1.08
Chemokine (C-C motif) ligand 2/monocyte chemotactic protein-1 Chemokine (C-C motif) ligand 1	CCL2(MCP-1)	*JE*	3890±739	3928±600	1.01
	I-309 (CCL1, TCA3)	*CCL1*	1149±85	996±35	0.87
Chemokine (C-C motif) ligand 5	CCL5/RANTES	*CCL5*	1118±81	1264±512	1.13
Chemokine (C-C motif) ligand 11/ Eotaxin	Eotaxin/CCL11	*CCL11*	1561±112	1091±345	0.69
Chemokine (C-C motif) ligand 12	CCL12/MCP-5	*CCL12*	1579±587	1100±348	0.69
Chemokine (C-C motif) ligand 17	CCL17/TARC	*CCL17*	2270±1034	1811±539	0.79
Chemokine (C-X-C motif) ligand 1 (melanoma growth stimulating activity, alpha) Chemokine (C-X-C motif) ligand 2	KC/CXCL1	*CXCL1*	4204±594	3117±724	0.74
	MIP-2/CXCL2	*CXCL2*	1092±168	1303±440	1.19
Chemokine (C-X-C motif) ligand 10	CXCL10/IP-10/CRG2	*CXCL10*	1682±158	2058±706	1.22
Chemokine (C-X-C motif) ligand 11	CXCL11/I-TAC	*CXCL11*	1002±96	895±119	0.89
Chemokine (C-X-C motif) ligand 12	SDF-1/CXCL-12	*CXCL12*	1565±410	2112±754	1.34
Colony stimulating factor 1 (macrophage)	M-CSF	*CFS1*	4311±700	4137±1060	0.96
Granulocyte-macrophage colony-stimulating factor	GM-CSF	*CSF2*	1428±684	772±351	0.54
Granulocyte colony stimulating factor	G-CSF	*CSF3*	1855±373	1095±65	0.59
Interferon gamma Interleukin 1α	IFN-γ	*IFNG*	4727±901	4527±903	0.96
	IL-1α/IL-1F1	*IL-1A*	2805±480	1901±194	0.68

Protein	Abbreviation	Gene	Mean Pixel Density		Ratio
			WT	KO	KO/WT
Interleukin 1β Interleukin 2	IL-1β/IL-1F2	*IL-1B*	2235±575	1246±172	0.56
	IL-2	*IL-2*	2886±772	1887±366	0.65
Interleukin 3	IL-3	*IL-3*	2648±234	1960±418	0.74
Interleukin 4	IL-4	*IL-4*	4955±566	3794±775	0.77
Interleukin 6	IL-6	*IL-6*	1639±712	1513±695	0.93
Interleukin 7	IL-7	*IL-7*	4595±1732	3665±1125	0.79
Interleukin 10 Interleukin 13	IL-10	*IL-10*	1430±644	1042±501	0.73
	IL-13	*IL-13*	4483±718	3061±346	0.68
Interleukin 16	IL-16	*IL-16*	3993±559	4174±446	1.05
Interleukin 23	IL-23	*IL-23*	2166±531	1298±176	0.59
Interleukin 27	IL-27	*IL-27*	2876±587	2084±367	0.72
TIMP metallopeptidase inhibitor 1	TIMP-1	*TIMP1*	10359±65	9890±447	0.95
Tumor necrosis factor alpha	TNFα/TNFSF2	*TNF*	2518±310	2683±594	1.07

Summary of Serum Cytokine Profile Changes of WT Mice w/wo TIC

Table 3.

Cytokine ratios for TNFR1/2 KO and WT mice 10 weeks after TIC injury

Protein	Abbreviation	*Gene*	Mean Pixel Density		Ratio
			WT	KO	KO/WT
Chemokine (C-C motif) ligand 4/ Macrophage inflammatory protein-1β	CCL4/MIP-1β	*CCL4*	513±175	2049±1144	4.0
Chemokine (C-C motif) ligand 12	CCL12/MCP-5	*CCL12*	1100±348	1811±873	1.65
Chemokine (C-C motif) ligand 17	CCL17/TARC	*CCL17*	1811±539	3670±1798	2.0
Chemokine (C-X-C motif) ligand 9/ Monokine induced by gamma interferon	CXCL9/MIG	*CXCL9*	1114±235	2172±568	1.95
Granulocyte-macrophage colony-stimulating factor	GM-CSF	*CFS2*	772±351	1833±997	2.38
Granulocyte colony stimulating factor	G-CSF	*CSF3*	1095±65	2752±753	2.5
IL-1 receptor antagonist	IL-1ra	*IL1RN*	4443±1399	2917±870	1.53
Interleukin 1α	IL-1α	*IL1A*	1901±194	5017±680	2.64**
Interleukin 1β	IL-1β/IL-1F2	*IL1B*	1246±172	1976±676	1.60
Interleukin 2	IL-2	*IL-2*	1887±366	2848±661	1.51
Interleukin 5	IL-5	*IL-5*	220±69	1832±675	8.30
Interleukin 12	IL-12/p70	*IL12A*	238±86	389±176	1.63
Interleukin 17	IL-17	*IL-17*	1460±250	2905±826	1.99
Interleukin 23	IL-23	*IL-23*	1298±176	3647±1707	2.81
Tumor necrosis factor alpha	TNF-α	*TNF*	2683±594	5167±493	1.93*
Interleukin 6	IL-6	*IL6*	1513±695	825±159	0.5
B lymphocyte chemoattractant	BLC/CXCL13/BCA1	*CXCL13*	2182±511	2059±720	0.94
Chemokine (C-C motif) ligand 2/monocyte chemotactic protein-1	CCL2(MCP1)	*JE*	3928±600	3915±514	0.99
C5a anaphylatoxins/Complement component 5	C5a	*C5*	5968±228	5345±271	0.9
Chemokine (C-C motif) ligand 1	I-309(CCL1, TCA3)	*CCL1*	996±35	1098±74	1.1
Chemokine (C-C motif) ligand 3/ Macrophage inflammatory protein-1α	CCL3/MIP-1α	*CCL3*	403±91	438±104	0.58
Chemokine (C-C motif) ligand 5	CCL5/RANTES	*CCL5*	1264±512	1105±286	0.87
Eotaxin/Chemokine (C-C motif) ligand 11	Eotaxin (CCL11)	*CCL11*	1091±345	1590±885	1.46
Chemokine (C-X-C motif) ligand 1/ melanoma growth stimulating activity alpha	KC/CXCL1	*CXCL1*	3117±724	3332±495	1.07
Chemokine (C-X-C motif) ligand 2	MIP2/CXCL2	*CXCL2*	1303±440	759±171	0.58
Chemokine (C-X-C motif) ligand 10	CXCL10/IP10/CRG-2	*CXCL10*	2058±706	1976±455	0.96

Protein	Abbreviation	Gene	Mean Pixel Density		Ratio
			WT	KO	KO/WT
Chemokine (C-X-C motif) ligand 11	CXCL11/I-TAC	*CXCL11*	895±119	996±180	1.11
Chemokine (C-X-C motif) ligand 12	SDF-1/CXCL12	*CXCL12*	2112±754	2758±650	1.3
Colony stimulating factor 1 (macrophage)	M-CSF	*CFS1*	4137±1060	4661±578	1.13
Interferon gamma	IFN-γ	*IFNG*	4527±903	4558±878	1.0
Interleukin 3	IL-3	*IL-3*	1960±418	2826±738	1.44
Interleukin 4	IL-4	*IL-4*	3794±775	4469±1288	1.18
Interleukin 7	IL-7	*IL-7*	3665±1125	5369±2271	1.47
Interleukin 10	IL-10	*IL-10*	1042±501	1482±828	1.42
Interleukin 13	IL-13	*IL-13*	3061±346	3195±421	1.04
Interleukin 16	IL-16	*IL16*	4174±446	5747±846	1.38
Interleukin 27	IL-27	*IL27*	2084±367	2510±463	1.2
TIMP metallopeptidase inhibitor 1	TIMP-1	*TIMP1*	9890±447	9845±399	1.0
Triggering receptor expressed on myeloid cells1	TREM-1	*TREM1*	5810±826	3958±165	0.68